Am J Transl Res 2019;11(8):4761-4775
www.ajtr.org /ISSN:1943-8141/AJTR0097308

*Original Article*

# Sp1-induced upregulation of the long noncoding RNA TINCR inhibits cell migration and invasion by regulating miR-107/miR-1286 in lung adenocarcinoma

Ya-Wen Gao[1*], Fang Ma[1*], Yang-Chun Xie[1], Meng-Ge Ding[1], Li-Hua Luo[2], Shun Jiang[1], Le Rao[1], Xian-Ling Liu[1]

*[1]Department of Oncology, The Second Xiangya Hospital of Central South University, Changsha 410011, Hunan, China; [2]Cancer Center, Union Hospital, Tongji Medical College, Huazhong University of Science and Technology, Wuhan 430022, Hubei, China. [*]Equal contributors.*

Received May 21, 2019; Accepted July 19, 2019; Epub August 15, 2019; Published August 30, 2019

**Abstract:** Long non-coding RNA tissue differentiation-inducing non-protein coding (TINCR) is associated with the carcinogenesis of several cancers. However, little is known about the function and mechanism of TINCR in lung adenocarcinoma (LUAD). Here, we aimed to analyze expression of TINCR and elucidate its mechanistic involvement in the progression of LUAD. The expression of TINCR was investigated according to Gene Expression Profiling Interactive Analysis at first and then detected in 29 LUAD tissues and paired adjacent normal tissues using qRT-PCR. Results indicated that TINCR was evidently downregulated in LUAD. The association between TINCR and clinicopathological parameters was analyzed by Pearson's chi-square test, suggesting TINCR was closely correlated with TNM stage and lymph mode metastasis. Subsequently, the function role of TINCR was examined by gain- and loss-of-function studies in LUAD (A549 and NCI-H292) cells. As analyzed by the scratch wound-healing and transwell assays, results revealed that TINCR suppressed the migration and invasion of A549 and NCI-H292 cells. However, TINCR exerted no effects on the cell proliferation as determined by CCK8 assay. Furthermore, we reported that loss of Sp1 could inhibit TINCR expression. Expressions of miR-107/miR-1286 were detected by qRT-PCR assay in A549 and NCI-H292 cells after TINCR knockdown or overexpression. In addition, the direct binding ability of the predicted miR-107 or miR-1286 binding site on TINCR was validated by luciferase activity assay. Results indicated TINCR could constrain the expression of miR-107/miR-1286, and was a target of them in LUAD cells. Bioinformatics analyses showed that BTRC and RAB14 was the potential target gene of miR-107 and miR-1286, respectively. These data revealed a possible regulatory mechanism in which upregulation of TINCR induced by Sp1 could constrain the migration and invasion through regulating miR-107 or miR-1286 in LUAD cells. Conjointly, our findings provide a valuable insight into the regulatory mechanism of TINCR in LUAD, supportive to its potential of therapeutic target for LUAD patients.

**Keywords:** TINCR, lung adenocarcinoma, miR-107, miR-1286, Sp1, progression

## Introduction

Lung cancer is the leading cause of cancer-related deaths worldwide, making it a major global health problem [1]. Carcinomas of non-small cell type represent approximately 85-90% of all new lung cancer diagnoses [2, 3]. These carcinomas are further classified into several major histological subtypes as following: lung adenocarcinoma (LUAD), adenosquamous cell carcinoma, squamous cell carcinoma, large cell carcinoma, and sarcomatoid carcinoma [4]. Among these types, LUAD is the most common with an increasing frequency [5]. However, the mechanisms underlying LUAD have not yet been completely elucidated.

Long non-coding RNAs (lncRNAs) are regulatory molecules with a length of more than 200 nucleotides, with limited protein-coding capacity [6]. Mounting evidence has indicated that they play roles in various biological processes such as cell multiplication, gene expression, and differentiation [7]. In addition, emerging evidence suggests that lncRNAs are associated with the pathogenesis and progression of human diseases, especially in tumors [8]. Various differentially expressed lncRNAs play vital roles in different tumors, and can be used

as diagnostic and prognostic biomarkers [9, 10]. This is evident in the case of LINC01512 in LUAD [11], antisense non-coding RNA in the INK4 locus (ANRIL) in gastric cancer [12], TCONS_00006195 in hepatocellular carcinoma [13], NF-KappaB Interacting LncRNA (NKILA) in non-small cell lung cancer [14].

Tissue differentiation-inducing non-protein coding RNA (TINCR), a 3.7-kb lncRNA located on human chromosome 19, is required for stabilizing mRNA for key differentiation genes [15]. Assembling evidence suggests that aberrant expression of TINCR is closely associated with a variety of human cancers. An example of this is the study carried out by Xu, et al. in which TINCR contributes to the oncogenic potential of gastric cancer [16]. This is also evident in the case that loss of TINCR expression promotes the proliferation and metastasis in colorectal cancer [17]. In addition, the existing reports about the role of TINCR in lung cancer [18, 19], breast cancer [20], esophageal squamous cell carcinoma [21] are strongly supportive. However, little is known about the function and mechanism of TINCR in the progression of LUAD.

In this study, we aimed to investigate the function role and preliminary regulatory mechanism of TINCR in LUAD. Firstly, the expression profiling of TINCR was predicted in LUAD and in its different stages according to Gene Expression Profiling Interactive Analysis (GEPIA), and then analyzed in 29 LUAD tissues compared with paired adjacent normal tissues. The association between TINCR and clinicopathological parameters was also evaluated. Secondly, the functional role of TINCR in the proliferation, migration and invasion of LUAD cells was assessed. Finally, the regulatory mechanism of TINCR in LUAD was preliminarily explored.

## Materials and methods

### *GEPIA analysis*

GEPIA is a web server for cancer and normal gene expression profiling and interactive analyses [22]. To determine the aberrant expression of TINCR, we investigated TINCR expression in LUAD tissues and adjacent normal tissues from GEPIA (http://gepia.cancer-pku.cn/detail.php?gene=TINCR) with following criteria in Column of Expression DIY-Profile: Gene, TINCR; Differential Methods, ANOVA; $|Log_2FC|$ Cutoff, 1; q-value Cutoff, 0.01; Log Scale, No; Dataset (Cancer name), LUAD; Plot Width, 12. In addition, TINCR expression in LUAD at different stages (stage I, II, III, IV) was visualized in GEPIA (http://gepia.cancer-pku.cn/detail.php?gene=TINCR) with following criteria in Column of Expression DIY-Stage plot: Gene, TINCR; Use major stage, Yes; Datasets Selection (Cancer name), LUAD; Log Scale, Yes.

The correlation between TINCR and Sp1 in LUAD tissues or adjacent normal tissues was analyzed from GEPIA (http://gepia.cancer-pku.cn/detail.php?gene=TINCR) with following criteria in Column of Correlation: Gene A: TINCR, Gene B: Sp1; Correlation Coefficient: Spearman; Used Expression Datasets: TCGA Tumor or TCGA Normal. As for the case of TINCR and BTRC or RAB14, the criteria of Gene B was BTRC or RAB14. The remaining sets were the same to the abovementioned.

### *Protein-protein interaction (PPI) network construction for the potential targets of miR-107/miR-1286*

The picTar (https://pictar.mdc-berlin.de/cgi-bin/PicTar_vertebrate.cgi), miRanda (http://www.microrna.org/microrna/home.do), Targetscan (http://www. targetscan.org/vert_72/), RNA22 (http://www.mybiosoftware.com/rna22-2-v2-microrna-target-detection.html), were applied to explore potential targets for miR-107. miRDB (http://mirdb.org/), and Targetscan (http://www. targetscan.org/vert_72/), were employed to evaluate potential targets for miR-1286. The potential targets for miR-107 or miR-1286 were obtained by the overlap of respective databases selected. The freely accessible Search Tool for the Retrieval of Interacting Genes (STRING) database (http://string-db.org) contains established and predicted PPI [23]. The potential targets were mapped onto the web-based tool STRING to generate a PPI network. The nodes and edges independently represented proteins and their interactions. Cytoscape (http://www.cytoscape.org/) [24] was employed to visualize these networks.

### *Patients and samples*

With the informed consents of all patients, a total of 29 cases of LUAD tissues and adjacent normal tissues were collected from LUAD patients undergoing surgical resection in the

Second Xiangya Hospital of Central South University. Fresh clinical tissue samples were immediately stored in liquid nitrogen for analysis. None of the patients had received anti-tumor therapy before diagnose. This study was ratified by the Research Ethic Committee of the Second Xiangya Hospital of Central South University.

*Cell culture and transfection*

The human LUAD cell lines A549 and NCI-H292 were purchased from Cell Bank of Type Culture Collection of Chinese Academy of Sciences (CBTCCCAS, Shanghai, China). They were cultured in Dulbecco's Modifed Eagle's Medium (DMEM; Thermo Fisher Scientifc, Waltham, MA, USA) supplemented with 10% fetal bovine serum in a humidified atmosphere of 5% (v/v) $CO_2$ at 37°C.

To overexpress TINCR, the coding sequence region of human TINCR was amplified and cloned into pcDNA3.1 vector (Invitrogen, Carlsbad, CA, USA) to produce pcDNA-TINCR. For knockdown of TINCR or Sp1, the small interfering RNAs (siRNAs) targeting TINCR or Sp1, and negative control (NC) siRNA were purchased from Ribobio (Guangzhou, China). They were labeled as si-TINCR, si1-Sp1, si2-Sp1 and NC, respectively. The target sequences of siRNAs were as follows: si-TINCR, 5'-GCAGAGTCATCACTACCTT-3' (sense); si1-Sp1, 5'-CCAACAGATTATCACAAAT-3' (sense); si2-Sp1, 5'-AAGCGCTTCATGAGGAGTG-3' (sense). The miR-107/miR-1286 mimic or inhibitor, which were synthesized and obtained from RiboBio (Guangzhou, China), were transfected into A549 cells to separately generate miR-107/miR-1286 overexpression or knockdown model. A549 and NCI-H292 cells were plated in 6-well plates for 24 hours (h), followed by being transfected with indicated siRNAs or plasmids using Lipofectamine 2000 (Invitrogen) in accordance with the manufacturer's instructions. Approximately 48 h after transfection, cells were collected for the following assays. Transfection efficiency was evaluated by quantitative real-time polymerase chain reaction (qRT-PCR) assay.

*RNA extraction and qRT-PCR assay*

Total RNA was isolated from indicated tissues or cells by Trizol reagent (Invitrogen, Carlsbad, CA) according to the manufacturer's instructions. Afterwards, TINCR, Sp1, BTRC or RAB14 was reversely transcribed to a single-stranded cDNA using Reverse Transcription System Kit (Takara, Dalian, China). Reverse transcription of miRNA-107 or miR-1286 was performed using miRNA First-Stand cDNA Synthesis Kit (GeneCopoeia, Guangzhou, China). qRT-PCR assay was performed by using SYBR Premix Ex Taq (Takara Biotech, Japan) on an ABI 7900 system (Applied Biosystems, Foster City, CA, USA). The housekeeping gene glyceraldehyde 3-phosphate dehydrogenase (GAPDH) was used as an internal control to normalize expression levels of genes, and U6 was used as an internal reference for miR-107 and miR-1286.

The relative quantification of TINCR, Sp1, miR-107 and miR-1286 were calculated by the $2^{-\Delta\Delta Ct}$ method. The PCR primers designed for genes are shown as below: GAPDH, forward 5'-ACGGATTTGGTCGTATTGGGCG-3' and reverse 5'-GCTCCTGGAAGATGGTGATGGG-3'; TINCR, forward 5'-GATCTCAC TCCAGGGTCTG-3' and reverse 5'-GAGTGTCTGAAGCAGTGTG-3'; Sp1, forward 5'-GTCCGCCCTCTGACCAAGAT-3' and reverse 5'-AAGGCACCACCACCATTACC-3'; BTRC, forward 5'-CCTGCGCCTGAGAGGTAAGA-3' and reverse 5'-CACAGAGACCTGGGCATAGA-3'; RAB14, forward 5'-TGGCAGTGTTTGGGGACATT-3' and reverse 5'-CAGCAGGTAAGCAACAGTGC-3'; U6, forward 5'-CTCGCTTCGGCAGCACA-3' and reverse 5'-AACGCTTCACGAATTTGCGT-3'; miR-107, forward 5'-AGCAGCATTGTACAGGGCTATCA-3' and reverse 5'-GCGAGCACAGAATTAATACGAC-3'; miR-1286, forward 5'-TGCAGGACCAAGATGAGCCCT-3' and reverse 5'-GCGAGCACAGAATTAATACGAC-3'.

*Cell proliferation assay*

A Cell Counting Kit-8 (CCK-8) assay was employed to evaluate the proliferative ability of A549 and NCI-H292 cells. Transfected cells (NC or si-TINCR; pcDNA 3.1 or TINCR) were cultured in 96-well plates and incubated for 24, 48 and 72 h. Optical density values were measured using the CCK-8 solution (Beyotime Institute of Biotechnology, Shanghai, China) in accordance with the manufacturer's protocol. Each group was repeated three times independently. The absorbance values at each point were measured at 450 nm.

*Cell migration assay*

The scratch wound-healing assay and transwell assay were employed to evaluate the migratory ability of A549 and NCI-H292 cells. For the scratch wound-healing assay, cells were plated

on 6-well plates and scraped by a pipette tip to generate uniform wounds prior to transfection (NC or si-TINCR; pcDNA3.1 or TINCR). Each well was washed thrice with PBS to remove floating cells. The initial distance (0 h) and the distances traveled by cells after 24, 48, and 72 h of scratching were detected microscopically at a magnification of 200× for each group. For transwell assay, transfected cells suspended in serum-free medium were added to the upper chamber at 37°C. Meanwhile, the modified Eagle medium containing 10% fetal bovine serum was added to the lower chamber. After 48 h of incubation at 37°C, cells remaining on the upper membrane were removed by cotton tip carefully, and adherent to underside of the membrane were fixed in 4% polyoxymethylene and stained with 1% crystal violet. The stained cells (migrated cells) were visualized in random fields using an optical microscope at a magnification of 200× for each group.

*Cell invasion assay*

The transwell assay to assess cell invasive ability was performed using Matrigel invasion chambers (BD Biosciences, Franklin Lakes, New Jersey, USA) according to the manufacturer's instructions. Transfected cells suspended in serum-free medium were added to the upper chamber pretreated by Matrigel at 37°C for 2 h. The following steps were in accordance with aforementioned transwell assay. The stained cells (invaded cells) were visualized in random fields using an optical microscope. Each experiment was performed in triplicate.

*Luciferase reporter assay*

The partial sequences of TINCR untranslated region (3'UTR) containing wide-type (WT) or mutant-type (MUT) miR-107/miR-1286 binding sites were cloned into the pGL3-Basic luciferase vector (Promega, Madison, WI, USA) to generate TINCR WT and TINCR MUT. The constructed luciferase vectors were subsequently transfected into A549 and NCI-H292 cells along with pRL-TK vector (Promega, Madison, WI, USA) and miR-NC/miR-107/miR-1286, respectively. The luciferase activities were measured 48 h post-transfection.

*Statistical analysis*

All data normally distributed were expressed as mean ± standard deviation. Student's t-test and one-way ANOVA analysis were employed to assess significant difference of different groups. A *P*-value < 0.05 was considered to be statistically significant. The correlation between TINCR expression and clinicopathologic features of LUAD patients was examined by *Pearson's chi-square* test. All statistical analyses were performed using the SPSS software (version 18.0, SPSS Inc., Chicago, IL, USA).

## Results

*TINCR is downregulated in LUAD tissues and correlates with lymph mode metastasis and TNM stage*

To explore the role of TINCR in LUAD, expression of TINCR was assessed according to GEPIA (http://gepia.cancer-pku.cn/detail.php?gene=TINCR), which is a visual database of The Cancer Genome Atlas (TCGA). As illustrated in **Figure 1A**, TINCR was significantly down-regulated expressed in LUAD tissues compared to adjacent normal tissues. In addition, significant difference was observed in the TINCR expression of LUAD tissues at different stage. Next, the expression profile of TINCR was analyzed using qRT-PCR in 29 LUAD tissues compared with paired adjacent normal tissues. Results indicated that TINCR was evidently downregulated in LUAD tissues compared with paired adjacent normal tissues (**Figure 2B**, $P < 0.01$). Then we explored the association between TINCR and clinicopathological parameters. As shown in **Table 1**, TINCR expression was not correlated with age, gender, smoking status and histology, but associated with TNM stage or lymph node metastasis ($P < 0.05$). Taken together, these findings revealed that TINCR is downregulated in LUAD tissues and correlates with TNM stage and lymph mode metastasis.

*TINCR exerts no effects on the proliferation of LUAD cells*

To investigate the effect of TINCR in LUAD, the proliferative ability of A549 and NCI-H292 cells were detected by CCK-8 assay at first. Expression of TINCR in A549 and NCI-H292 cells transfected with si-TINCR was significantly reduced, while that in those cells transfected with pcDNA-TINCR was evidently increased (**Figure 2A**, **2B**, $P < 0.05$, $P < 0.01$, $P < 0.001$). These results indicated that TINCR was effectively knocked down or overexpressed after siRNA or pcDNA treatment. Results of CCK-8 assay presented that no significant difference was observed in the proliferative ability of A549

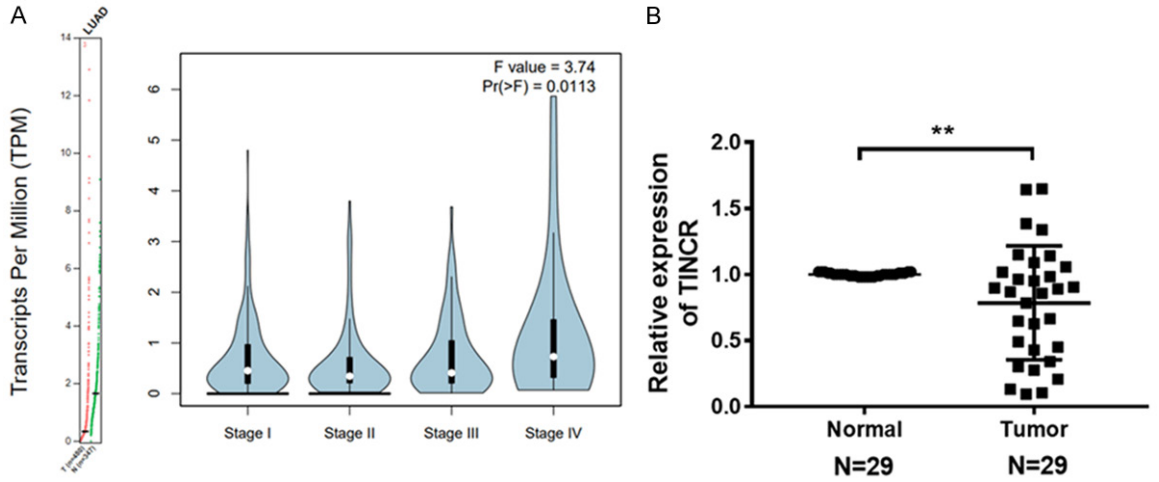


**Figure 1.** TINCR is low expressed in LUAD tissues. A. TINCR was low expressed in LUAD tissues (Left panel), and its expression profiling in LUAD at different stage was visualized (Right panel) according to GEPIA (http://gepia.cancer-pku.cn/detail.php?gene=TINCR). B. TINCR was significantly downregulated in 29 LUAD tissues compared with paired adjacent normal tissues as analyzed by qRT-PCR. Data shown are mean ± standard deviation. Statistically significant differences are indicated as **, $P < 0.01$; student's t-test. The experiment was repeated at least three times. TINCR, tissue differentiation-inducing non-protein coding RNA; LUAD, lung adenocarcinoma; GEPIA, Gene Expression Profiling Interactive Analysis; qRT-PCR, quantitative real-time polymerase chain reaction.

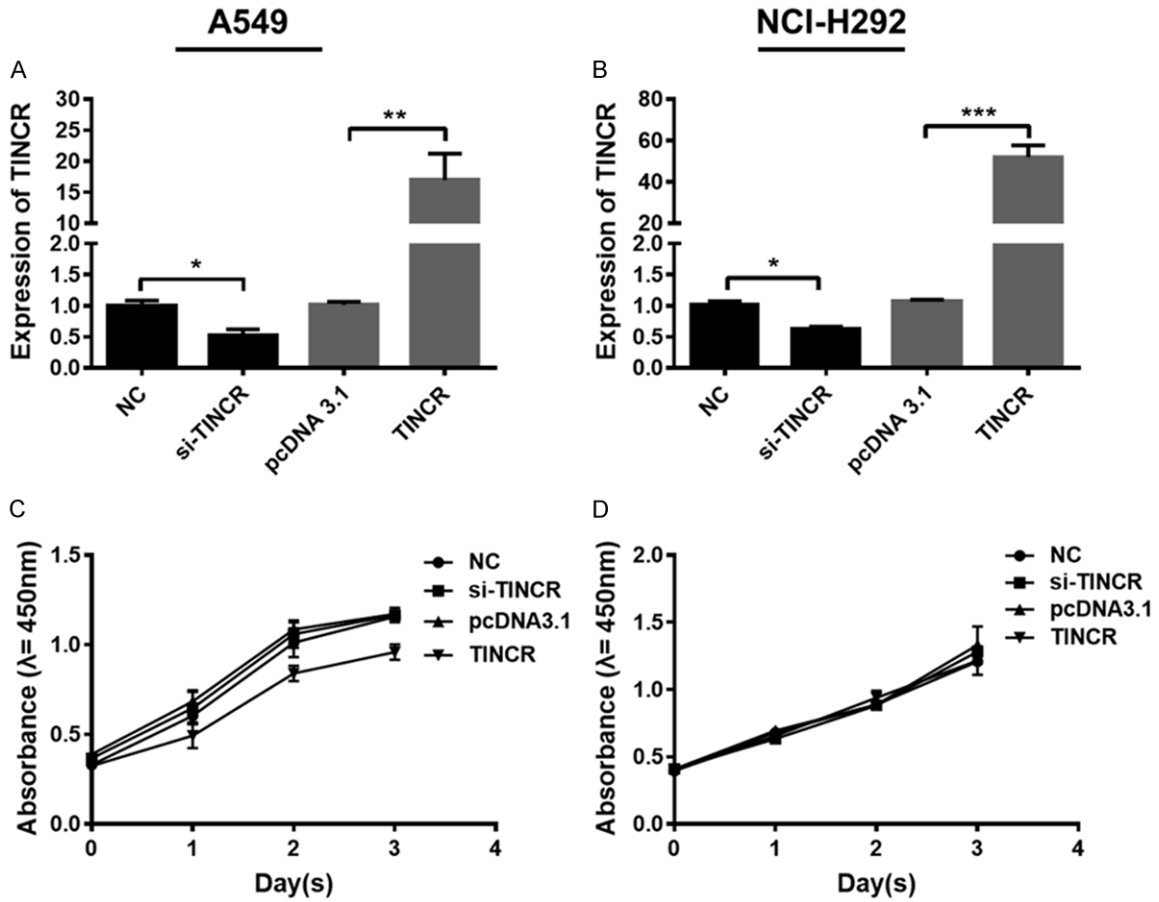


**Figure 2.** TINCR exerts no effects on the proliferation of LUAD cells. A, B. Expression of TINCR was determined by qRT-PCR in A549 and NCI-H292 cells after treated with si-TINCR, pcDNA-TINCR or NC, respectively. C, D. The

proliferation of A549 and NCI-H292 cells treated with si-TINCR, pcDNA-TINCR or NC was detected by CCK-8 assay, respectively. Data shown are mean ± standard deviation. Statistically significant differences are indicated as *, $P < 0.05$, **, $P < 0.01$; student's t-test. The experiment was repeated at least three times. TINCR, tissue differentiation-inducing non-protein coding RNA; LUAD, lung adenocarcinoma; qRT-PCR, quantitative real-time polymerase chain reaction; NC, negative control; siRNA, small interfering RNA; CCK-8, cell counting kit-8.

**Table 1.** Correlation between TINCR expression and clinicopathologic features of LUAD patients

| Parameters | TINCR expression | | | *P* value |
|---|---|---|---|---|
| | High | Low | Total | |
| | N = 11 (37.93%) | N = 18 (62.07%) | N = 29 | |
| *Age (years)* | | | | |
| < 63 | 5 (17.24%) | 12 (41.38%) | 17 | 0.2688 |
| ≥ 63 | 6 (20.69%) | 6 (20.69%) | 12 | |
| *Gender* | | | | |
| Male | 8 (27.59%) | 15 (51.73%) | 23 | 0.9391 |
| Female | 3 (10.34%) | 3 (10.34%) | 6 | |
| *Histology* | | | | |
| Squamous | 2 (6.90%) | 3 (10.34%) | 5 | 0.3612 |
| Adenocarcinoma | 9 (31.03%) | 15 (51.73%) | 24 | |
| *Smoking Status* | | | | |
| Current-smokers | 7 (24.14%) | 12 (41.38%) | 19 | 0.8700 |
| Never-smokers | 4 (13.79%) | 6 (20.69%) | 10 | |
| *TNM Stage* | | | | |
| I/II | 3 (10.35%) | 18 (62.07%) | 21 | 0.0484 |
| III/IV | 4 (13.79%) | 4 (13.79%) | 8 | |
| *Lymph mode metastasis* | | | | 0.0374 |
| Presence | 4 (13.79%) | 2 (6.90%) | 8 | |
| Absence | 5 (17.24%) | 18 (62.07%) | 21 | |

*P*-values were calculated by *Pearson's chi-square* test.

and NCI-H292 cells transfected with si-TINCR in comparison with NC group (**Figure 2C**, **2D**). Similar results were obtained in the case of cells transfected with pcDNA-TINCR (**Figure 2C**, **2D**). Taken together, these results revealed that TINCR exerts no effects on the proliferation of LUAD cells.

*TINCR suppresses the migration and invasion of LUAD cells*

In order to investigate the function role of TINCR in LUAD, experiments regarding TINCR overexpression and knockdown were performed in A549 and NCI-H292 cells to determine their migratory and invasive abilities. Both the scratch wound-healing and transwell assays were employed to detect cell migration. The scratch wound-healing assay showed that the migratory rate of A549 cells transfected with si-TINCR was significantly attenuated at 48 and 72 h comparable to NC group (**Figure 3A**, $P < 0.05$, $P < 0.001$). Conversely, the migratory rate of A549 cells transfected with pcDNA-TINCR was obviously facilitated at 48 and 72 h comparable to NC group (**Figure 3A**, $P < 0.05$). Similar results were obtained in the case of NCI-H292 cells (**Figure 3B**, $P < 0.05$, $P < 0.01$). Additionally, the transwell assay revealed the migratory capacity of A549 and NCI-H292 cells transfected with si-TINCR was strengthened comparable to NC group, while that of those cells with pcDNA-TINCR was weakened comparable to NC group (**Figure 3C**, **3D**). The Matrigel assay indicated that siRNA treatment evidently promoted the invasive capacity of A549 and NCI-H292 cells compared to NC group, while pcDNA treatment had an opposite effect (**Figure 3E**, **3F**). Collectively, these data indicated that TINCR suppresses the migration and invasion of LUAD cells.

*Knockdown of Sp1 suppresses the expression of TINCR in LUAD cells*

Reportedly, Sp1 regulated the expression of TINCR through binding its promoter region in gastric cancer [16], breast cancer [20], and colorectal cancer [25]. According to GEPIA database (http://gepia.cancer-pku.cn/detail.php?gene=TINCR), the correlation between TINCR and Sp1 in LUAD tissues and adjacent normal tissues was analyzed. As presented in **Figure 4A**, TINCR correlated with Sp1 expression in LUAD tissues (*p*-value = 1.7e-05; Spearman). Subsequently, in order to investigate the effect of Sp1 on TINCR expression in

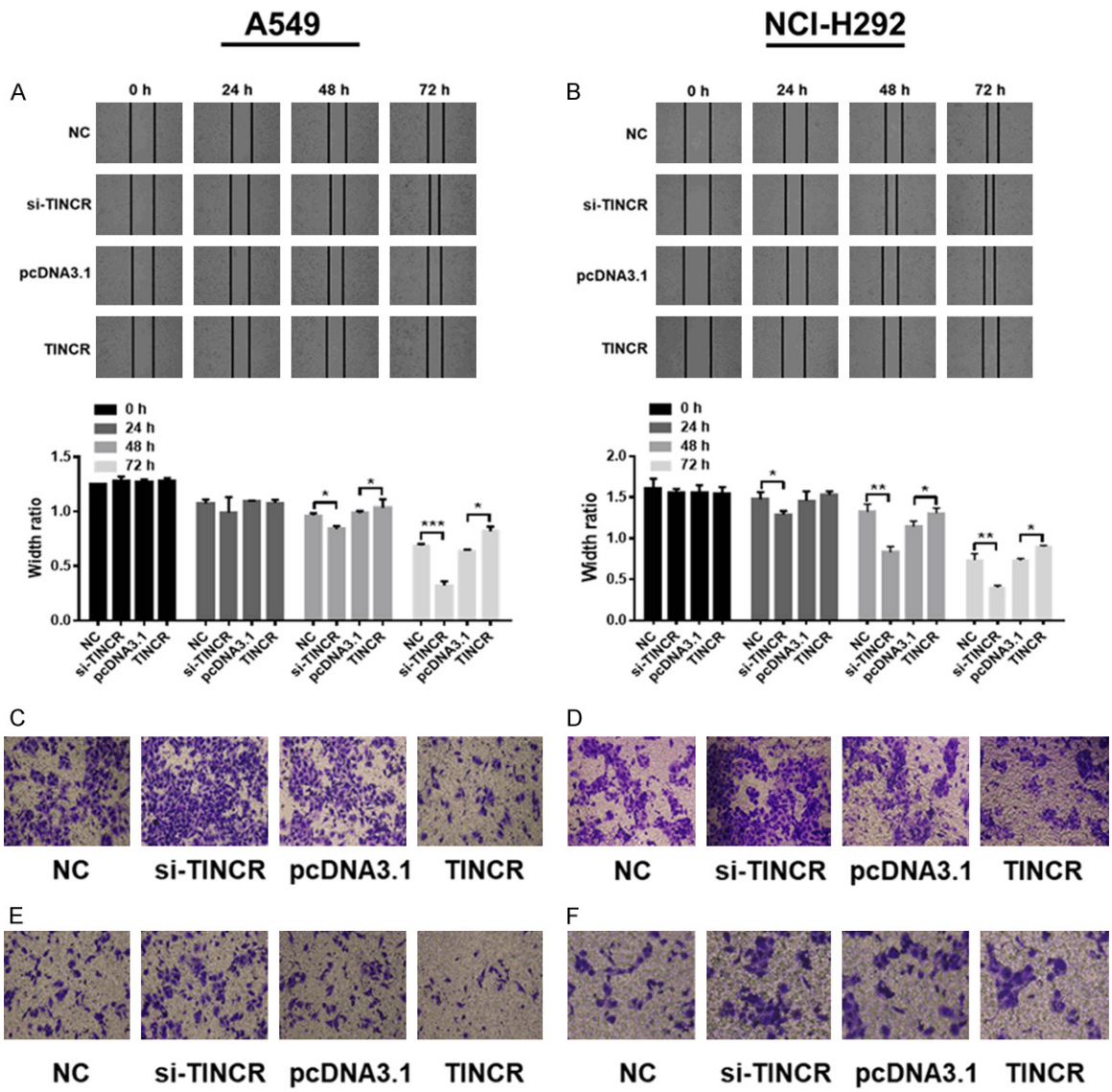


**Figure 3.** TINCR constrains the migration and invasion of LUAD cells. A, B. The migratory rate of A549 and NCI-H292 cells transfected with si-TINCR or pcDNA-TINCR were evaluated by the scratch wound-healing assay. C, D. The migratory capacity of A549 and NCI-H292 cells transfected with si-TINCR or pcDNA-TINCR for 48 h were analyzed by the transwell assay. E, F. The invasive capacity of A549 and NCI-H292 cells transfected with si-TINCR or pcDNA-TINCR for 48 h were assessed by the transwell assay. Each image was taken at 200× magnification. Data shown are mean ± standard deviation. Statistically significant differences are indicated as *, $P < 0.05$, **, $P < 0.01$, ***, $P < 0.001$; student's t-test. The experiment was repeated at least three times. TINCR, tissue differentiation-inducing non-protein coding RNA; NC, negative control; siRNA, small interfering RNA; h, hour.

LUAD, two specific siRNAs were designed and synthesized to inhibit Sp1, and then TINCR expression were examined. A549 and NCI-H292 cells were transfected with NC or siRNA targeting Sp1 (si1-Sp1, si2-Sp1). As analyzed by qRT-PCR, expression of Sp1 was effectively knocked down when cells transfected with si1-Sp1 (**Figure 4B**, **4C**, $P < 0.01$, $P < 0.001$). In details, si-Sp1 in NCI-H292 cells showed better efficiency than in A549 (**Figure 4B**, **4C**). Similarly, expression of TINCR was significantly decreased when A549 and NCI-H292 cells transfected with si1-Sp1 as detected by qRT-PCR (**Figure 4D**, **4E**, $P < 0.05$). However, no obvious difference was obtained in the expression of TINCR in A549 and NCI-H292 cells transfected with si2-Sp1 compared to NC (**Figure 4D**, **4E**). Collectively, si1-Sp1 exhibits better efficiency and downregulation of Sp1 suppresses the expression of TINCR.

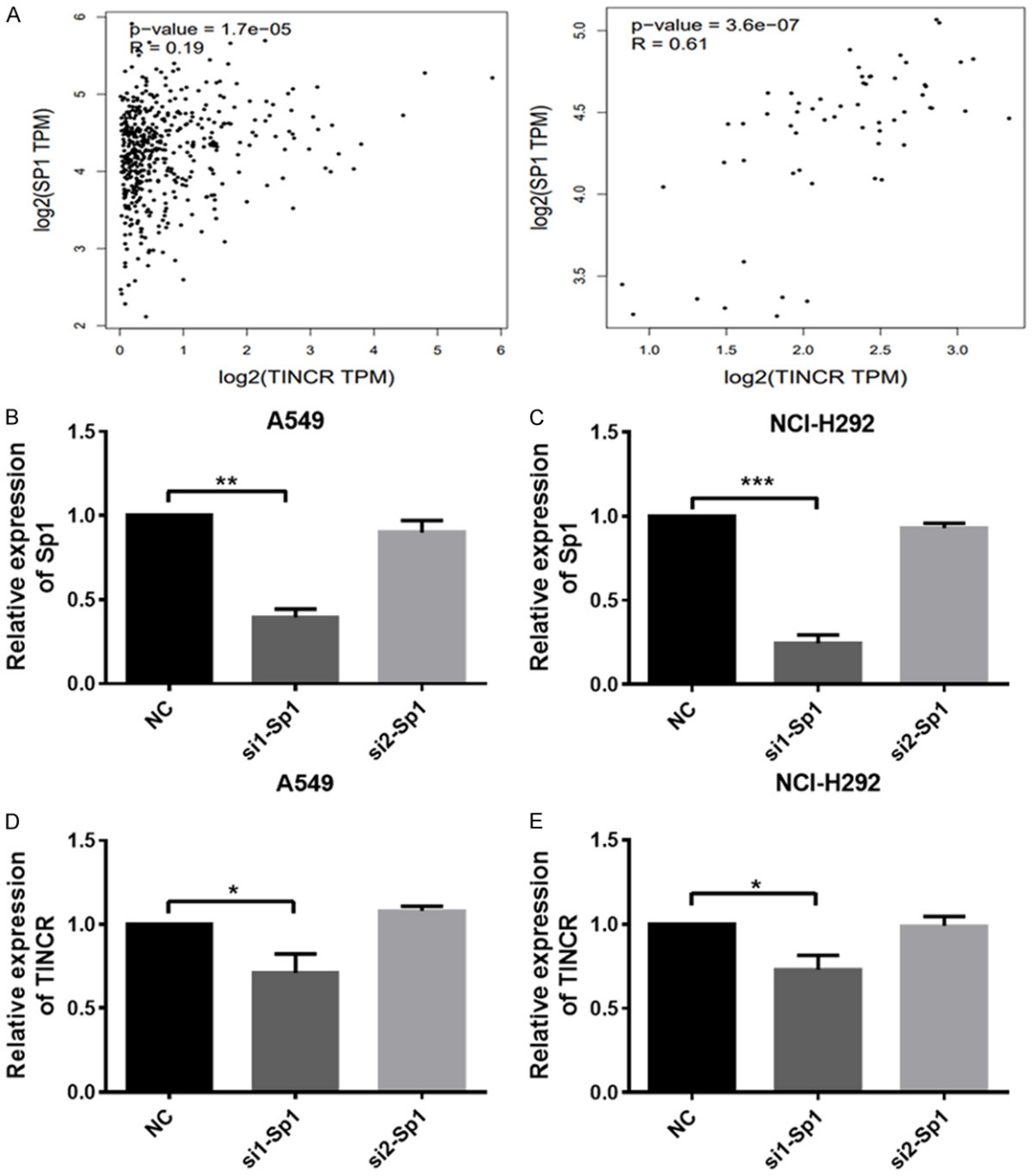


**Figure 4.** Downregulation of Sp1 suppresses the expression of TINCR. A. The correlation between TINCR and Sp1 in LUAD tissues (Left panel) and adjacent tissues (Right panel) was analyzed according to GEPIA database (http://gepia.cancer-pku.cn/detail.php?gene=TINCR). B, C. Sp1 expression in A549 and NCI-H292 cells after transfection of NC (siRNA negative control) or si1-Sp1, si2-Sp2. D, E. TINCR expression in A549 and NCI-H292 cells after transfection of NC (siRNA negative control) or si1-Sp1, si2-Sp2. Data shown are mean ± standard deviation. Statistically significant differences are indicated as *, $P < 0.05$, **, $P < 0.01$, ***, $P < 0.001$; student's t-test. The experiment was repeated at least three times. TINCR, tissue differentiation-inducing non-protein coding RNA; NC, negative control; siRNA, small interfering RNA.

*TINCR inhibits the expression of miR-107/miR-1286, and is a target of them in LUAD cells*

To investigate the association of TINCR with miR-107/miR-1286, expressions of miR-107/miR-1286 were detected by qRT-PCR assay in A549 and NCI-H292 cells after TINCR knockdown or overexpression. As shown in **Figure 5A**, knockdown of TINCR by transfection with si-TINCR led to obviously increased expressions

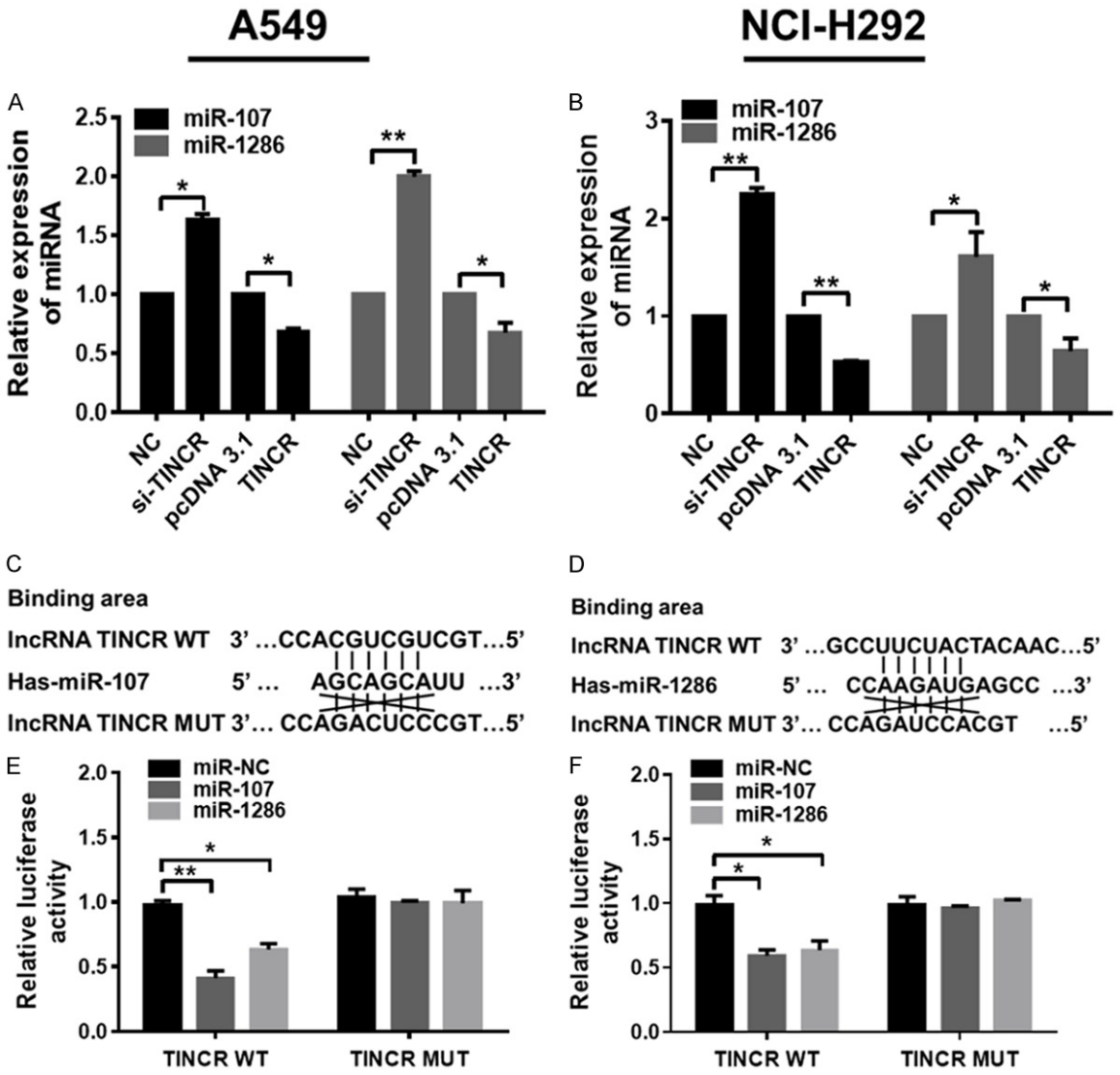


**Figure 5.** TINCR constrains the expression of miR-107 and miR-1286, and is a target of them in LUAD cells. A, B. Relative expressions of miR-107 and miR-1286 were analyzed by qRT-PCR analysis in A549 and NCI-H292 cells transfected with NC, si-TINCR, pcDNA3.1 and pcDNA-TINCR, respectively. C. Predicted binding sites between miR-107, D. miR-1286 and WT /MUT TINCR using the online software programs TargentScan (http://www.targetscan.org/mamm_31/) and starBase (http://starbase.sysu.edu.cn/); E, F. luciferase activity of the indicated group in A549 and NCI-H292 cells transfected with pRL-TK vector + miR-NC/miR-107/miR-1286 + TINCR WT, or pRL-TK vector + miR-NC/miR-107/miR-1286 + TINCR MUT. Data shown are mean ± standard deviation. Statistically significant differences are indicated as *, $P < 0.05$, **, $P < 0.01$; student's t-test and one-way ANOVA analysis. The experiment was repeated at least three times. TINCR, tissue differentiation-inducing non-protein coding RNA; miR, microRNA; LUAD, lung adenocarcinoma; qRT-PCR, quantitative real-time polymerase chain reaction; NC, negative control; siRNA, small interfering RNA; MUT, mutant type; WT, wild type.

of miR-107 ($P < 0.05$) and miR-1286 ($P < 0.05$), while overexpression of TINCR by transfection with TINCR pcDNA contributed to evidently decreased expressions of miR-107 ($P < 0.01$) and miR-1286 ($P < 0.05$) in A549 cells. Moreover, similar results were observed in NCI-H292 cells (**Figure 5B**, $P < 0.05$, $P < 0.01$).

On the basis of the aforementioned results, we further investigate the correlation between TINCR and miR-107/miR-1286 in LUAD cells. Using the online software programs starBase (http://starbase.sysu.edu.cn/) and TargentScan (http://www.targetscan.org/mamm_31/), results revealed that both miR-107 (**Figure 5C**) and miR-1286 (**Figure 5D**) formed complementary base pairings with TINCR. There existed putative miR-107-binding and miR-1286-binding sites in 3'UTR of TINCR (**Figure 5C**, **5D**). Luciferase reporter vectors were therefore con-

structed to confirm the direct target between TINCR and miR-107/miR-1286. The luciferase activity was detected in A549 and NCI-H292 cells after co-transfecting with TINCR WT, pRL-TK vector and miR-NC/miR-107/miR-1286, or TINCR MUT, pRL-TK vector and miR-NC/miR-107/miR-1286. As a result, luciferase activity was remarkably lower in miR-107 + TINCR-WT group and miR-1286 + TINCR-WT group compared to miR-NC group in both A549 and NCI-H292 cells (**Figure 5E**, **5F**, $P < 0.05$, $P < 0.01$). However, no significant difference was observed in the luciferase activity of miR-107 + TINCR MUT group and miR-1286 + TINCR MUT group compared to miR-NC group in both A549 and NCI-H292 cells (**Figure 5E**, **5F**). Taken together, these results indicated that TINCR inhibits the expression of miR-107/miR-1286, and is a target of them in LUAD cells.

*Predictive targets of miR-107/miR-1286 according to bioinformatics analyses*

In order to explore the potential miR-107/miR-1286-related mechanism in LUAD, their possible targets were predicted according to bioinformatics analyses. Four databases, picTar (https://pictar.mdc-berlin.de/cgi-bin/PicTar_vertebrate.cgi), miRanda (http://www.microrna.org/microrna/home.do), Targetscan (http://www. targetscan.org/vert_72/), and RNA22 (http://www.mybiosoftware.com/rna22-v2-microrna-target-detection.html), were applied to explore potential targets for miR-107. We obtained 46 potentials targets according to the overlap of every database (**Figure 6A**), which was listed in Supplementary Table 1. With an aim to explore the interactive relationship of these 46 potential targets, they were mapped to STRING online database (https://string-db.org/cgi/input.pl). Their PPI network was visualized and shown in **Figure 6B** (Left panel). Subsequently, hub genes were obtained and screened by Cytoscape software (version 3.4.0, available online: http://www.cytoscape.org/) according to degree score, as presented in **Figure 6B** (Right panel). The hub gene BTRC achieved the highest degree score (= 6.000), indicating it was the target gene of miR-107 most likely.

As for the prediction of potential targets for miR-1286, only two databases, miRDB (http://mirdb.org/), and Targetscan (http://www.targetscan.org/vert_72/), were therefore employed because of its few studies. We obtained 474 potentials targets according to the overlap of two databases (**Figure 6A**), which was listed in Supplementary Table 2. The following analyses were similar to the case of miR-107. The PPI network of the top-100 potential targets was visualized and shown in **Figure 6C** (Left panel) and hub genes were obtained and screened by Cytoscape software (version 3.4.0, available online: http://www.cytoscape.org/) according to degree score (**Figure 6C**, right panel). The hub gene RAB14 achieved the highest degree score (= 3.443), indicating it was the target gene of miR-1286 most likely.

Based on the above prediction, the verification in vitro for the screened targets of miR-107 and miR-1286 was performed. Namely, the effect of miR-107/miR-1286 on the expression level of BTRC/RAB14 was evaluated in A549 cells. As displayed in **Figure 6D**, the expression level of BTRC was significantly reduced in miR-107 mimic group compared to NC mimic group ($P < 0.01$), while that was augmented in miR-107 inhibitor group compared to NC inhibitor group ($P < 0.001$). Similar results were obtained in the case of the expression level of RAB14 detected after miR-1286 overexpression or knockdown (**Figure 6E**, $P < 0.05$, $P < 0.01$). These indicated that miR-107 could target BTRC and miR-1286 could target RAB14. Next, the correlation between TINCR and BTRC, TINCR and RAB14 in LUAD tissues and adjacent normal tissues was analyzed according to GEPIA database (http://gepia.cancer-pku.cn/detail.php?gene=TINCR). Results presented in **Figure 6F**, **6G** showed that TINCR correlated with BTRC or RAB14 expression in LUAD tissues ($p$-value = 9.6e-05; $p$-value = 0.0027; Spearman). Taken together, these results indicated that BTRC or RAB14 might be a target of miR-107 or miR-1286, which was involved in the progression of LUAD.

## Discussion

Countless improvements have been achieved in the understanding of molecular mechanisms of LUAD development and progression, however, the specific mechanisms of LUAD still remain largely unknown [26]. LncRNAs are largely reported to be dysregulated in many types of human cancers. Many dysregulated lncRNAs have also been identified in LUAD [11, 27, 28].

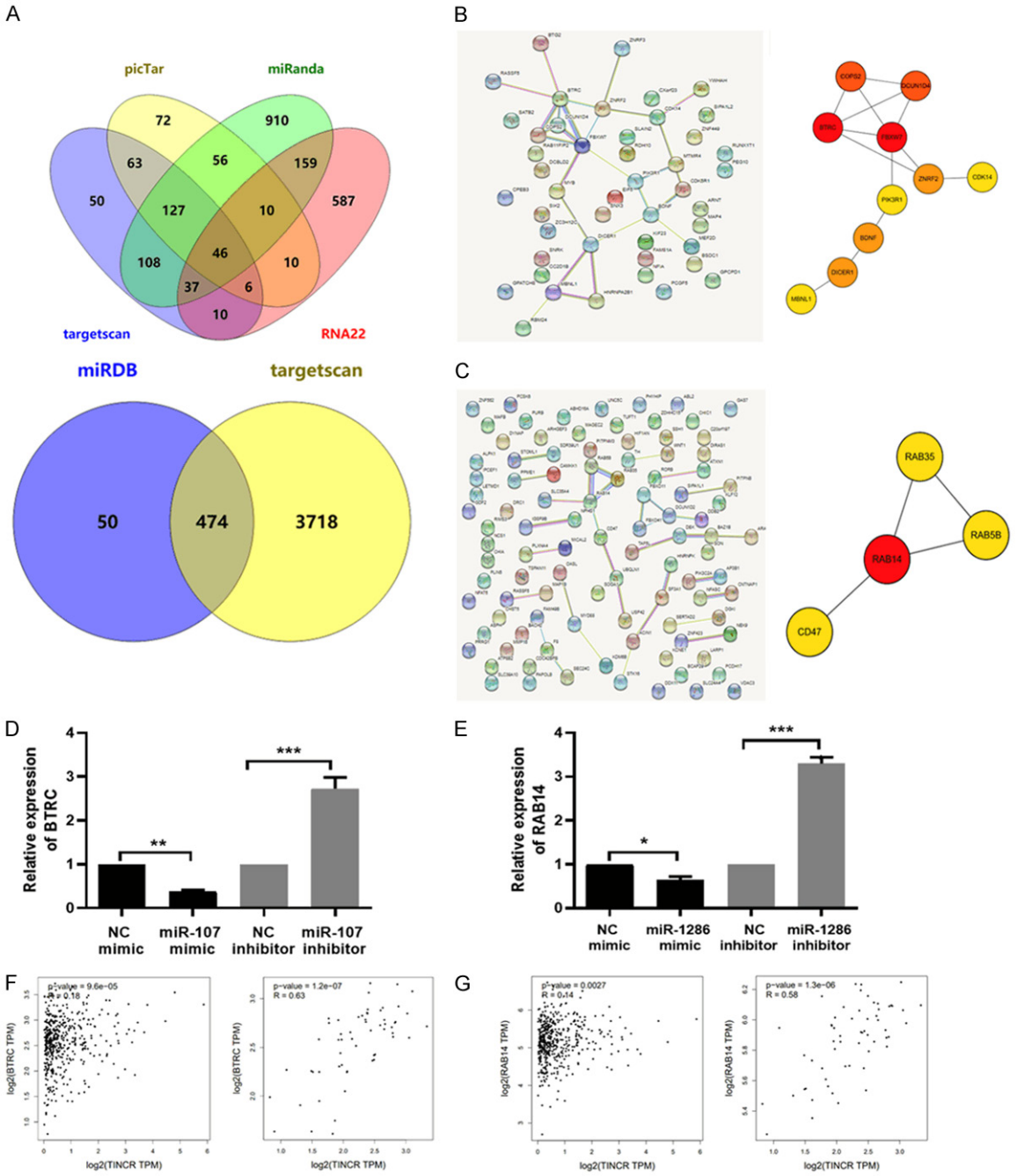


**Figure 6.** The targets of miR-107/miR-1286 were predicted according to bioinformatics analyses and verified in LUAD cells. (A) Venn diagram showed the overlap of potential targets for miR-107 (Upper panel) in picTar, miRanda, Targetscan, and RNA22 databases, or miR-1286 (Lower panel) in miRDB and Targetscan databases. (B) The PPI network was constructed and visualized for the 46-potential targets of miR-107 (Left panel), (C) for the top-100-potential targets of miR-1286 (Left panel). Top hub genes were obtained and screened by Cytoscape software (version 3.4.0, available online: http://www.cytoscape.org/) according to degree score (Right panel). The line between two nodes shows the interaction between two genes. The deeper of node color indicates higher degree score. (D) The expression of BTRC was detected by qRT-PCR assay in A549 cells transfected with miR-107/NC mimic or miR-107/NC inhibitor. (E) The expression of RAB14 was detected by qRT-PCR assay in A549 cells transfected with miR-1286/NC mimic or miR-1286/NC inhibitor. (F) The correlation between TINCR and BTRC, (G) TINCR and RAB14 in LUAD tissues (Left panel) and adjacent tissues (Right panel) was analyzed according to GEPIA database (http://gepia.cancer-pku.cn/detail.php?gene=TINCR). Data shown are mean ± standard deviation. Statistically significant differences are indicated as *, $P < 0.05$, **, $P < 0.01$, ***, $P < 0.001$; student's t-test. The experiment was repeated

at least three times. miR, microRNA; PPI, protein-protein interaction; TINCR, TINCR, tissue differentiation-inducing non-protein coding RNA; BTRC, beta-transducin repeat containing E3 ubiquitin protein ligase; RAB14, member RAS oncogene family; qRT-PCR, quantitative real-time polymerase chain reaction; NC, negative control; LUAD, lung adenocarcinoma; GEPIA, Gene Expression Profiling Interactive Analysis.

As previous reported, TINCR exerts discrepant effects in various cancers. For example, Tong peng Xu, et al. reported that TINCR was aberrantly expressed in gastric cancer, and E2F1/TINCR/STAU1/CDKN2B signaling axis contributed to the oncogenic potential of gastric cancer [29]. Zhang ZY, et al. revealed that TINCR was statistically downregulated in colorectal cancer, and its loss promoted the proliferation and metastasis of colorectal cancer through activating EpCAM cleavage [17]. Notably, recent literature has emerged that offers contradictory findings about the role of TINCR in lung cancer. This is exemplified in the study conducted by Zhijun Zhu, et al. [21], which reported that TINCR was upregulated in non-small cell lung cancer and promoted NSCLC tumorigenesis and progression via BARF-activated MAPK pathway [19]. Conversely, Xiaochun Liu, et al. pointed out that TINCR expression was downregulated in lung cancer and suppressed proliferation and invasion through regulating miR-544a/FBXW7 axis in lung cancer [18]. In this study, we found TINCR was downregulated in LUAD tissues on the basis of GEPIA database coupled with the detection in 29 LUAD patients. In addition, TINCR expression was closely correlated with TNM stage or lymph node metastasis.

To further reveal the function role of TINCR, a series of tests were performed in LUAD cell lines A549 and NCI-H292. Results indicated that TINCR overexpression led to an obvious repression in migration and invasion, while TINCR knockdown resulted in an evident promotion of migration and invasion in LUAD cells. However, neither TINCR overexpression nor knockdown contributed to the proliferation of LUAD cells, different from the results of the inhibitory role of TINCR in lung cancer cell lines A549 and H460, reported by Xiaochun Liu et al. [18]. This may be attributed to the different source of cell lines, cell passage number and cellular state.

Sp1 is a transcription factor and reported to promote cancer progression through altering the expression of other genes. This is evident in the case that Guanghua Liu, et al. indicated that Sp1 bound to the lncRNA-SNHG14 promoter region and promoted its transcription [30]. In fact, Sp1 binding to TINCR promoter region to alter its expression has been demonstrated in gastric cancer [16], breast cancer [20], and colorectal cancer [25]. On the basis of GEPIA database, TINCR correlated with Sp1 expression in LUAD tissues. Afterwards, we found that knockdown of Sp1 resulted in the decreased expression of TINCR in LUAD cells. This conveyed information that Sp1 could alter TINCR expression in LUAD.

Mounting evidence has recently shown a novel regulatory mechanism between lncRNAs and miRNAs-lncRNAs serve endogenous molecular sponges to compete for miRNAs, thus negatively regulating miRNA expression [31]. For example, TP73-AS1 promotes breast cancer proliferation through miR-200a-mediated TFAM inhibition [32]. The lncRNA MEG3 functions as a competing endogenous RNA of miR-181s to regulate the progression of gastric cancer [33]. Intriguingly, an integrated analysis of lncRNA competing interactions in human gastric cancer demonstrated that TINCR probably functions as ceRNA with numerous potential miRNAs [34]. We therefore speculated that this regulatory mechanism existed in LUAD. According to bioinformatics databases (starBase and TargetScan), we found miR-107 and miR-1286 that may interact with TINCR. The regulating relationship between TINCR and miR-107 or miR-1286 was confirmed based on the following: 1) overexpression of TINCR contributed to evidently decreased expressions of miR-107 and miR-108, while knockdown of TINCR had an opposite effect; 2) the direct binding ability of the predicted miR-107 or miR-1286 binding site on TINCR was validated by luciferase activity assay. In fact, the regulating relationship between TINCR and miR-107 has been demonstrated in colorectal cancer [35]. MiR-107 has been identified as a critical role in lung cancer [36, 37]. However, what is less clear is the function role of miR-1286 in various cancers. Next, the targets of miR-107/miR-1286 were predicted according to bioinformat-

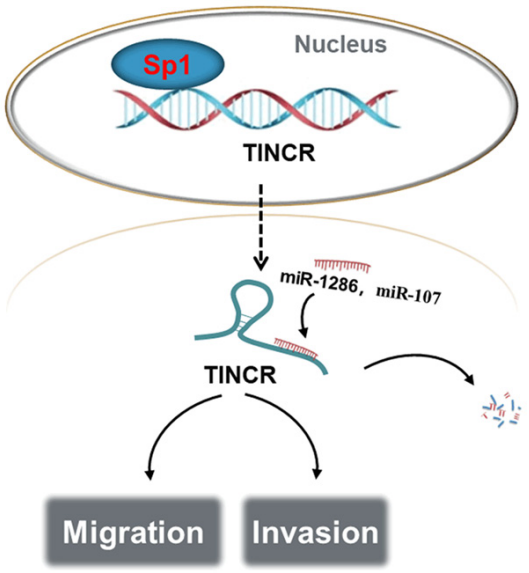


**Figure 7.** Schematic model of Sp1-induced upregulation of TINCR inhibits cell migration and invasion by regulating miR-107/miR-1286 in LUAD. TINCR, tissue differentiation-inducing non-protein coding RNA; miR, microRNA; LUAD, lung adenocarcinoma.

ics analyses and verified in LUAD cells. miR-107 downregulated the expression of BTRC and miR-107 downregulated the expression of RAB14. Moreover, TINCR correlated with BTRC or RAB14 expression in LUAD tissues according to GEPIA database. Our results revealed that BTRC or RAB14 was a target of miR-107 or miR-1286 to be involved in the progression of LUAD, which provided the direction of further research. As illustrated in **Figure 7**, these data, while preliminary, suggested a possible regulatory mechanism in which upregulation of TINCR induced by Sp1 could constrain the migration and invasion through regulating miR-107 or miR-1286 in LUAD cells.

Despite these promising results, few limitations characterizing this study cannot be ignored. For example, the regulatory mechanism of Sp1 on TINCR in LUAD remains unclear; the verification of BTRC or RAB14 as a target of miR-107 or miR-1286 by different methods is worth exploring; the function role of miR-107 or miR-1286 in LUAD is currently unclear. Further studies, which take these aspects into account, will need to be undertaken.

In conclusion, our findings offer insight into a possible mechanism of TINCR in LUAD and suggest TINCR might be used as a new biomarker and therapeutic target for LUAD patients.

## Acknowledgements

This work was supported by the National Key Research and Development Program of China (2016YFC1201800).

## Disclosure of conflict of interest

None.

**Address correspondence to:** Xian-Ling Liu, Department of Oncology, The Second Xiangya Hospital of Central South University, No. 139 Renmin Road, Changsha 410000, Hunan, China. E-mail: liuxianling@csu.edu.cn

## References

[1] Altorki NK, Markowitz GJ, Gao D, Port JL, Saxena A, Stiles B, McGraw T and Mittal V. The lung microenvironment: an important regulator of tumour growth and metastasis. Nat Rev Cancer 2019; 19: 9-31.

[2] Gridelli C, Rossi A, Carbone DP, Guarize J, Karachaliou N, Mok T, Petrella F, Spaggiari L and Rosell R. Non-small-cell lung cancer. Nat Rev Dis Primers 2015; 1: 15009.

[3] Ettinger DS, Akerley W, Bepler G, Blum MG, Chang A, Cheney RT, Chirieac LR, D'Amico TA, Demmy TL, Ganti AK, Govindan R, Grannis FW Jr, Jahan T, Jahanzeb M, Johnson DH, Kessinger A, Komaki R, Kong FM, Kris MG, Krug LM, Le QT, Lennes IT, Martins R, O'Malley J, Osarogiagbon RU, Otterson GA, Patel JD, Pisters KM, Reckamp K, Riely GJ, Rohren E, Simon GR, Swanson SJ, Wood DE, Yang SC; NCCN Non-Small Cell Lung Cancer Panel Members. Non-small cell lung cancer. J Natl Compr Canc Netw 2010; 8: 740-801.

[4] Travis WD, Brambilla E, Noguchi M, Nicholson AG, Geisinger KR, Yatabe Y, Beer DG, Powell CA, Riely GJ, Van Schil PE, Garg K, Austin JH, Asamura H, Rusch VW, Hirsch FR, Scagliotti G, Mitsudomi T, Huber RM, Ishikawa Y, Jett J, Sanchez-Cespedes M, Sculier JP, Takahashi T, Tsuboi M, Vansteenkiste J, Wistuba I, Yang PC, Aberle D, Brambilla C, Flieder D, Franklin W, Gazdar A, Gould M, Hasleton P, Henderson D, Johnson B, Johnson D, Kerr K, Kuriyama K, Lee JS, Miller VA, Petersen I, Roggli V, Rosell R, Saijo N, Thunnissen E, Tsao M, Yankelewitz D. International association for the study of lung cancer/american thoracic society/european respiratory society international multidisciplinary classification of lung adenocarcinoma. J Thorac Oncol 2011; 6: 244-285.

[5] Lee YS and Bae SC. How do K-RAS-activated cells evade cellular defense mechanisms? Oncogene 2015; 35: 827.

[6] Nagano T and Fraser P. No-nonsense functions for long noncoding RNAs. Cell 2011; 145: 178-181.
[7] Quan H, Liang M, Li N, Dou C, Liu C, Bai Y, Luo W, Li J, Kang F, Cao Z, Yang X, Jiang H and Dong S. LncRNA-AK131850 sponges MiR-93-5p in newborn and mature osteoclasts to enhance the secretion of vascular endothelial growth factor a promoting vasculogenesis of endothelial progenitor cells. Cell Physiol Biochem 2018; 46: 401-417.
[8] Tano K and Akimitsu N. Long non-coding RNAs in cancer progression. Front Genet 2012; 3: 219.
[9] Huarte M. The emerging role of lncRNAs in cancer. Nat Med 2015; 21: 1253.
[10] Qi P and Du X. The long non-coding RNAs, a new cancer diagnostic and therapeutic gold mine. Mod Pathol 2012; 26: 155-65.
[11] Chen J, Zhang F, Wang J, Hu L, Chen J, Xu G and Wang Y. LncRNA LINC01512 promotes the progression and enhances oncogenic ability of lung adenocarcinoma. J Cell Biochem 2017; 118: 3102-3110.
[12] Zhang EB, Kong R, Yin DD, You LH, Sun M, Han L, Xu TP, Xia R, Yang JS, De W and Chen J. Long noncoding RNA ANRIL indicates a poor prognosis of gastric cancer and promotes tumor growth by epigenetically silencing of miR-99a/miR-449a. Oncotarget 2014; 5: 2276-2292.
[13] Yu S, Li N, Huang Z, Chen R, Yi P, Kang R, Tang D, Hu X and Fan X. A novel lncRNA, TCONS_00006195, represses hepatocellular carcinoma progression by inhibiting enzymatic activity of ENO1. Cell Death Dis 2018; 9: 1184.
[14] Lu Z, Li Y, Wang J, Che Y, Sun S, Huang J, Chen Z and He J. Long non-coding RNA NKILA inhibits its migration and invasion of non-small cell lung cancer via NF-kappaB/snail pathway. J Exp Clin Cancer Res 2017; 36: 54.
[15] Kretz M. TINCR, staufen1, and cellular differentiation. RNA Biol 2013; 10: 1597-1601.
[16] Xu TP, Liu XX, Xia R, Yin L, Kong R, Chen WM, Huang MD and Shu YQ. SP1-induced upregulation of the long noncoding RNA TINCR regulates cell proliferation and apoptosis by affecting KLF2 mRNA stability in gastric cancer. Oncogene 2015; 34: 5648-5661.
[17] Zhang ZY, Lu YX, Zhang ZY, Chang YY, Zheng L, Yuan L, Zhang F, Hu YH, Zhang WJ and Li XN. Loss of TINCR expression promotes proliferation, metastasis through activating EpCAM cleavage in colorectal cancer. Oncotarget 2016; 7: 22639-22649.
[18] Liu X, Ma J, Xu F and Li L. TINCR suppresses proliferation and invasion through regulating miR-544a/FBXW7 axis in lung cancer. Biomed Pharmacother 2018; 99: 9-17.
[19] Zhu ZJ and He JK. TINCR facilitates non-small cell lung cancer progression through BRAF-activated MAPK pathway. Biochem Biophys Res Commun 2018; 497: 971-977.
[20] Liu Y, Du Y, Hu X, Zhao L and Xia W. Up-regulation of ceRNA TINCR by SP1 contributes to tumorigenesis in breast cancer. BMC Cancer 2018; 18: 367.
[21] Xu Y, Qiu M, Chen Y, Wang J, Xia W, Mao Q, Yang L, Li M, Jiang F, Xu L and Yin R. Long noncoding RNA, tissue differentiation-inducing nonprotein coding RNA is upregulated and promotes development of esophageal squamous cell carcinoma. Dis Esophagus 2016; 29: 950-958.
[22] Tang Z, Li C, Kang B, Gao G, Li C and Zhang Z. GEPIA: a web server for cancer and normal gene expression profiling and interactive analyses. Nucleic Acids Res 2017; 45: W98-W102.
[23] Szklarczyk D, Morris JH, Cook H, Kuhn M, Wyder S, Simonovic M, Santos A, Doncheva NT, Roth A, Bork P, Jensen LJ and von Mering C. The STRING database in 2017: quality-controlled protein-protein association networks, made broadly accessible. Nucleic Acids Res 2017; 45: D362-D368.
[24] Su G, Morris JH, Demchak B and Bader GD. Biological network exploration with Cytoscape 3. Curr Protoc Bioinformatics 2014; 47: 8.13.1-24.
[25] Yu S, Wang D, Shao Y, Zhang T, Xie H, Jiang X, Deng Q, Jiao Y, Yang J, Cai C and Sun L. SP1-induced lncRNA TINCR overexpression contributes to colorectal cancer progression by sponging miR-7-5p. Aging (Albany NY) 2019; 11: 1389-1403.
[26] Denisenko TV, Budkevich IN and Zhivotovsky B. Cell death-based treatment of lung adenocarcinoma. Cell Death Dis 2018; 9: 117.
[27] Dong HX, Wang R, Jin XY, Zeng J and Pan J. LncRNA DGCR5 promotes lung adenocarcinoma (LUAD) progression via inhibiting hsa-mir-22-3p. J Cell Physiol 2018; 233: 4126-4136.
[28] Deng J, Deng H, Liu C, Liang Y and Wang S. Long non-coding RNA OIP5-AS1 functions as an oncogene in lung adenocarcinoma through targeting miR-448/Bcl-2. Biomed Pharmacother 2018; 98: 102-110.
[29] Xu TP, Wang YF, Xiong WL, Ma P, Wang WY, Chen WM, Huang MD, Xia R, Wang R, Zhang EB, Liu YW, De W and Shu YQ. E2F1 induces TINCR transcriptional activity and accelerates gastric cancer progression via activation of TINCR/STAU1/CDKN2B signaling axis. Cell Death Dis 2017; 8: e2837.
[30] Liu G, Ye Z, Zhao X and Ji Z. SP1-induced up-regulation of lncRNA SNHG14 as a ceRNA promotes migration and invasion of clear cell renal cell carcinoma by regulating N-WASP. Am J Cancer Res 2017; 7: 2515-2525.
[31] Cesana M, Cacchiarelli D, Legnini I, Santini T, Sthandier O, Chinappi M, Tramontano A and

Bozzoni I. A long noncoding RNA controls muscle differentiation by functioning as a competing endogenous RNA. Cell 2011; 147: 358-369.

[32] Yao J, Xu F, Zhang D, Yi W, Chen X, Chen G and Zhou E. TP73-AS1 promotes breast cancer cell proliferation through miR-200a-mediated TFAM inhibition. J Cell Biochem 2018; 119: 680-690.

[33] Peng W, Si S, Zhang Q, Li C, Zhao F, Wang F, Yu J and Ma R. Long non-coding RNA MEG3 functions as a competing endogenous RNA to regulate gastric cancer progression. J Exp Clin Cancer Res 2015; 34: 79.

[34] Li CY, Liang GY, Yao WZ, Sui J, Shen X, Zhang YQ, Peng H, Hong WW, Ye YC, Zhang ZY, Zhang WH, Yin LH and Pu YP. Integrated analysis of long non-coding RNA competing interactions reveals the potential role in progression of human gastric cancer. Int J Oncol 2016; 48: 1965-1976.

[35] Zhang X, Yao J, Shi H, Gao B and Zhang L. LncRNA TINCR/microRNA-107/CD36 regulates cell proliferation and apoptosis in colorectal cancer via PPAR signaling pathway based on bioinformatics analysis. Biol Chem 2019; 400: 663-675.

[36] Cui J, Mo J, Luo M, Yu Q, Zhou S, Li T, Zhang Y and Luo W. c-Myc-activated long non-coding RNA H19 downregulates miR-107 and promotes cell cycle progression of non-small cell lung cancer. Int J Clin Exp Pathol 2015; 8: 12400-12409.

[37] Zhang Z, Zhang L, Yin ZY, Fan XL, Hu B, Wang LQ and Zhang D. miR-107 regulates cisplatin chemosensitivity of A549 non small cell lung cancer cell line by targeting cyclin dependent kinase 8. Int J Clin Exp Pathol 2014; 7: 7236-7241.

**Supplementary Table 1.** The list of 46 potential targets of miR-107

| Gene name |
|---|
| RUNX1T1 |
| DCBLD2 |
| DICER1 |
| ZNRF3 |
| PCGF5 |
| CDK14 |
| MBNL1 |
| CDK5R1 |
| EIF5 |
| HNRNPA2B1 |
| PEG10 |
| SIK2 |
| NFIA |
| BTG2 |
| CPEB3 |
| MAP4 |
| RBM24 |
| SLAIN2 |
| RDH10 |
| YWHAH |
| BTRC |
| MTMR4 |
| SATB2 |
| CXorf23 |
| SNX3 |
| KIF23 |
| FBXW7 |
| GPATCH8 |
| RASSF5 |
| DCUN1D4 |
| COPS2 |
| ZNF449 |
| ZNRF2 |
| MYB |
| CC2D1B |
| BDNF |
| GPCPD1 |
| MEF2D |
| PIK3R1 |
| RAB11FIP2 |
| SNRK |
| BSDC1 |
| ARNT |
| FAM81A |
| ZC3H12C |
| SIPA1L2 |

**Supplementary Table 2.** The list of 474 potential targets of miR-1286

| Gene name |
|---|
| MAFB |
| ALPK1 |
| NFAT5 |
| FBXO11 |
| MAP1B |
| SOGA1 |
| ATP8B2 |
| SEC24C |
| BACH2 |
| PURB |
| VDAC3 |
| HIF1AN |
| ACIN1 |
| PCDH17 |
| SON |
| TSPAN11 |
| MYD88 |
| UBQLN1 |
| ABHD16A |
| USP42 |
| TAF5L |
| DRC1 |
| CHIA |
| IPCEF1 |
| HNRNPK |
| PCSK6 |
| STK16 |
| KLF12 |
| RAB14 |
| STOML1 |
| PITPNM3 |
| GAS7 |
| ASPH |
| SLC35A4 |
| CHIC1 |
| RASSF5 |
| LARP1 |
| IGSF9B |
| C16orf47 |
| C20orf197 |
| DYNAP |
| NCS1 |
| ZNF423 |
| ARHGEF3 |
| SIPA1L1 |
| CHST5 |

SDR39U1
PLIN5
MICAL2
PHYHIP
SF3A1
RAB5B
DIRAS1
GDF2
KDM6B
CDC42BPB
LETMD1
RORB
ZNF562
ARAP2
DEK
SSH1
ZDHHC15
DGKI
SLC39A10
CAMKK1
BCAP29
MAGEC2
CD47
NEK9
WNT1
PPME1
DDX11
PLXNA4
FBXO41
ATXN1
MMP16
PITPNB
ABL2
SLC24A4
TH
AP3B1
RIMS3
SERTAD2
KCNE1
TUFT1
PRRG1
NPHS1
F8
NFASC
OASL
BAZ1B
PIK3C2A
PAPOLB
CNTNAP1

FAM49B
DDB2
RAB35
UNC5C
DCUN1D2
TEAD1
ASF1B
RAB11FIP1
FAAH
CNOT2
CCNYL1
SYT4
MRPL22
ATXN1L
PTPRJ
FAM155B
WNK3
SNTG2
DDX55
TNRC6C
TMEM132E
RB1CC1
RBM14
NAT9
DBNDD1
TXNDC17
CHRD
SKIDA1
KIAA0930
MIEF2
LGALSL
NOS1
LIMA1
ARL4C
NUDT7
AVPR2
WARS
CECR2
EBF2
ITPR2
APPBP2
UVRAG
PCP4
POM121
CPLX1
RASGEF1B
STIM2
CDCA5
SEC14L1

TLK1
ATP13A3
PHLDA3
SYVN1
BCL7A
NTNG2
NCOR1
CTSO
TMUB2
MAML2
DVL3
CCDC85C
CCNK
OPRK1
FOXP1
C19orf12
MAVS
PTPN5
ARL10
SAMD12
MEF2C
ZNF543
TMEM201
NGB
MAP3K7
RUNX1
CCR9
FAIM2
RCL1
NAIP
KIF21B
CHAF1A
PSMA5
EGLN3
CDKN2A
ZNF609
CAPZA1
FBXL19
TPCN2
PCYT1B
CNTD1
CAB39L
ATP11A
KRTAP5-7
AFF2
THRAP3
SMOX
SH2D4B
PCGF5

KRTAP5-9
ZNRF1
IDH3G
KIAA1143
CAMKV
PXDC1
CD68
ABHD15
PRDM15
NMNAT2
MTMR9
BTBD7
CALCA
RORA
ASH1L
MYO9A
MED13L
DOCK3
ABCB9
CSTF3
MAP3K11
KCNK3
TSPAN9
SLC7A14
ZAP70
AGO1
DAO
CSNK2B
HPCAL4
VPS26A
VPREB1
SLC38A1
PLEKHB2
SETD2
ELAVL2
GATA3
GALNT2
EXOSC2
GRIK3
PPP1R16A
KDM5B
PLA2G4C
ADPRHL1
PIK3AP1
RD3
SH3KBP1
VANGL1
ABHD14A
OTUD4

HMGN1
RABAC1
PIAS2
PISD
ATRN
RCC1
DPT
ZMAT3
USP3
ARSJ
ATP6AP1
DDX52
ICMT
CHEK1
RSL24D1
DOLPP1
IL2RB
CD6
TRIM39
KLHL36
KLF3
DNAJC13
LRPPRC
ALKBH1
STOML3
NTNG1
ATF2
GPATCH2
FCRLA
DDHD2
TMEM217
NFATC2
DLG2
RPS27L
PXT1
ASCC2
TMSB4Y
SLC26A4
KRT79
INSR
MR1
CPA4
MMP8
AMOTL1
ZNF770
ADAMTS19
AMER1
GMFB
SMIM12

DOCK4
TSPEAR
GAB3
KCNAB2
SWAP70
TSHR
CDS2
AAR2
TRHDE
MLXIP
PREP
CRISPLD1
FARSB
DPM2
NICN1
LCT
PTPRN2
SYNPO
ZFYVE27
FHL1
REG1B
STON1
TMEM107
TMEM198
STAT5B
SDK2
PNPLA5
HECA
SCRN1
APOLD1
HIPK1
HNRNPUL2
APOC3
GNAS
USP24
PMPCB
ROBO2
CTTNBP2NL
ELAC1
TFCP2L1
TNNI1
XIRP1
SPATA5
AP2A2
MFAP4
COBL
MGRN1
PRR16
HOPX

CASK
IGDCC3
CDK5R1
CASP2
BEST2
BSN
MCM4
SLC48A1
LDLRAD2
NOTCH3
BRD4
NLRC5
NIPSNAP1
FAM102A
SLC4A4
GTF3C4
FASN
NAP1L4
FZD1
PACS2
ACER1
C1orf226
PHC1
TIPIN
ZFP41
EGLN2
FBXO4
ORAI1
IRF8
EBPL
ITPR3
ALPK3
NF2
SZT2
GJA3
GABBR2
P4HA1
IGF2
MAP3K9
TBC1D5
MATN1
SPATA13
TMEM170B
XPNPEP3
CHD2
CNR1
GPR158
CRNN
CHTF8

ZIC5
FGF17
TAOK1
RPS6KA1
FASLG
AKNA
PNRC2
MMP10
CMTM4
LARS
IFITM2
GOLGA7B
ST3GAL1
STX16
ACVR2B
GRIN2A
MMEL1
CXorf40B
REEP3
POLE
ZNF736
MBNL2
IL12RB1
S1PR2
ACOX3
SHISA6
EMCN
WIPF2
TMEM64
WIPI2
RPL10
CAMK1D
SLC24A2
ELFN2
GSK3B
CAMK2A
ENTPD6
FZD8
SLC6A3
GGA2
TUBGCP3
NLK
LRP2
CEACAM1
ZMAT2
ADARB1
VPS53
COX6B2
CNRIP1

MTA3
TBC1D1
GOLGA1
LIN28A
SCAMP2
SH3BP2
PANK2
VAMP1
RNF115
AMMECR1L
AK4
GAP43
GALNTL6
GNPDA1
FER
PIK3R5
BIRC3
NCKIPSD
GSG1
SIAH3
CYTH3
DCAF7
TRIM25
GAL3ST3
REPS2
CWC25
HPCA
ZFYVE1
GPR63
GAS8
RAB3D
MXD1
TMEM33
MTMR3
CYBB
HESX1